Technical Material

Experimental analysis and uncertainty quantification using random sampling technique for ADS experiments at KUCA

Tomohiro Endo[a*], Go Chiba[b], Willem Frederik Geert van Rooijen[c],

Masao Yamanaka[d] and Cheol Ho Pyeon[d]

[a] *Graduate School of Engineering, Nagoya University, Furo-cho, Chikusa-ku, Nagoya 464-8603, Japan;*

[b] *Graduate School of Engineering, Hokkaido University, Kita 8, Nishi 5, Kita-ku, Sapporo, Hokkaido, 060-0808 Japan;*

[c] *Research Institute of Nuclear Engineering, University of Fukui, 1-2-4 Kanawa-cho, Tsuruga-shi, Fukui 914-0055, Japan;*

[d] *Research Reactor Institute, Kyoto University, 2 Asashiro-Nishi, Kumatori-cho, Sennan-gun, Osaka 590-0494 Japan*

Acknowledgements

This work was supported under the project of Basic Research for Nuclear Transmutation Techniques by Accelerator-Driven System, a Special Research Program funded by Chubu Electric Power Co., Inc. The authors are grateful to all the staff at KUCA and to the FFAG accelerator group for their assistance during the experiments.

Abstract

Nuclear data-induced uncertainties of neutronics parameters (neutron multiplication factor k_{eff}, one-point kinetics parameters and prompt neutron decay constant α) are quantified for lead-

*Corresponding author. Email: t-endo@energy.nagoya-u.ac.jp

bismuth zoned accelerator-driven system experiments at the Kyoto University Critical Assembly, in order to contribute validation for subcritical core analysis. The random sampling technique using SCALE6.2.1/Sampler/NEWT/PARTISN is utilized for the validation and the uncertainty quantification, because the random sampling technique is applicable for a problem which is not easy to apply the perturbation theory. Consequently, it is confirmed that the numerical results of α reasonably agree with the experimental ones, compared with the nuclear data-induced uncertainties. In addition, it is clarified that the nuclear data-induced correlations between α and k_{eff} and between α and neutron generation time Λ are strongly negative and positive, respectively. This fact implies that the numerical predictions of k_{eff} and Λ can be improved by the data assimilation technique using subcritical experimental results of α, which can be directly measured even for a deep subcritical system.

Keywords; KUCA; ADS; subcriticality; uncertainty quantification; random sampling technique; prompt neutron decay constant; one-point kinetics parameters; lead-bismuth

1. Introduction

The accelerator-driven system (ADS) has been investigated to reduce a burden of nuclear waste disposal by transmuting minor actinides and long-lived fission products. As basic researches on neutronics parameters in the source-driven subcritical system, a series of ADS experiments has been conducted at Kyoto University Critical Assembly (KUCA) [1-8].

As one of the KUCA ADS experiments, neutronics parameters such as prompt neutron decay constant and subcriticality (or negative reactivity) were measured for a ^{235}U-fueled and lead-bismuth (Pb-Bi) zoned core [7,8], where the material Pb-Bi is considered as a candidate material for the target and the coolant in the designed ADS. In this Pb-Bi zoned ADS experiment, the subcriticality deduced by the excess reactivity and the control rod worth was directly measured in near critical state where the one-point reactor approximation is assumed. For deep subcritical experimental cores where the numerically-estimated subcriticality ranges from 4812 to 11556 pcm, the subcriticality was not directly measured. Instead, the prompt neutron decay constant α was measured by the pulsed neutron source (PNS) method [9] and the Feynman-α method [10] using spallation neutrons generated by 100 MeV proton beam from the fixed-field alternating gradient (FFAG) accelerator [11,12]. These experimental results can be utilized for validation of a neutron transport code to predict neutronics parameters in a subcritical core, though, of course, continuous improvement of experimental core is necessary to acquire more effective integral experimental data for the designed ADS.

In the subcritical core analysis in ADS, the following neutronics parameters are numerically predicted by solving the conventional k_{eff}-eigenvalue problem: effective neutron multiplication factor k_{eff} and one-point kinetics parameters (effective delayed neutron fraction β_{eff}, prompt neutron lifetime ℓ, and neutron generation time Λ). From the view point of comparison with experimental results, the prompt neutron decay constant α is predicted by solving a different eigenvalue problem. In addition, the uncertainty quantification (UQ) is important to clarify the precision of predicted parameters; thus a practical method for UQ is

desirable. In the case of k_{eff}, the numerical methodology based on first-order perturbation theory is well established. Various code systems exist to perform the sensitivity analysis (SA) and UQ of k_{eff} in an automated way, *e.g.* SCALE6.2/TSUNAMI [13], SAGEP [14], MARBLE2 [15] and CBZ [16]. In the case of one-point kinetics parameters, their definition apparently corresponds to reactivity worth. Thus, the generalized perturbation theory (GPT) is mathematically applicable to the UQ of one-point kinetics parameters, though the cumbersome GPT calculations are necessary. To avoid the GPT calculations, the SA and UQ of β_{eff} can be estimated by two times conventional SA for k_{eff} and the prompt neutron multiplication factor $k_{\mathrm{eff},p}$, based on the k-ratio method [17,18]. Furthermore, the SA and UQ of Λ can be also estimated by two times conventional SA for k_{eff} and the perturbed neutron multiplication factor k'_{eff}, which is obtained for the perturbed system where absorption cross sections are increased by the reciprocal neutron velocity $\frac{1}{\mathrm{v}(E)}$ [19]. On the other hand, in the case of α, the practical method of SA and UQ of α is still not sufficiently established, because of the difference in eigenvalue problem between k_{eff} and α.

Recently, the random sampling technique has been effectively utilized for UQ [20-29], particularly for a problem which is not easy to apply the perturbation theory. As mentioned above, the SA and UQ of one-point kinetics parameters and α are not straightforward. The automated code system is uncommon; at least, the functions of SA and UQ of these kinetics parameters are not available in the recent version of SCALE code system. Therefore, the application of the random sampling technique is very practical for the UQ of kinetics parameters.

In this study, the first attempt was made to apply the random sampling technique to UQ of kinetics parameters for Pb-Bi zoned ADS experiments at the KUCA, with the combined use of SCALE6.2.1/Sampler/NEWT [13,21,30] and PARTISN codes [31]. Main purposes of this study are to verify the calculation procedure of UQ using the random sampling technique by comparing with the reference k_{eff}-uncertainty using SCALE6.2.1/TSUNAMI-3D [32]; and to investigate nuclear data-induced uncertainties of kinetics parameters and the correlation among

neutronics parameters through the experimental analysis for the Pb-Bi zoned ADS experiments at KUCA. Note that, the UQ was conducted only for 4 experimental cores where the control rod patterns are symmetry, due to limitations of calculation memory and time.

This paper is organized as follows: In **Section 2**, the target of experiment is briefly explained. **Section 3** describes the calculation condition and procedure for UQ using the random sampling technique, followed by the results and discussion of **Section 4**. Finally, concluding remarks are presented in **Section 5**.

2. Experiment

The ADS experiments were carried out in the A-core composed of the highly-enriched uranium-aluminum (HEU) fuel, polyethylene, and Pb-Bi plates [7,8]. **Figures 1** and **2** shows the core configurations and the loaded fuel assemblies, respectively.

<Figure 1>

<Figure 2>

There are three types of fuel assemblies. One is a normal fuel assembly "F," which consists of 36 unit cells (HEU 1/16" thick and polyethylene 3/8" thick). Another is a partial fuel assembly "16," which consist of 16 times of the same unit cells as "F." The other is a special Pb-Bi zoned fuel assembly "f," which consists of total number of 60 unit cells: 30 unit cells for central region (HEU 1/8" thick and Pb-Bi ~3.3 mm thick) and other 15+15 unit cells for upper and lower regions (HEU 1/8" thick and polyethylene 1/8" thick).

As shown in **Figure 1**, there are 6 cases of experimental cores by changing the number of "F" assemblies and the following control rod patterns:

Case 1: C1, C2, C3 are fully inserted; S4, S5, S6 are fully withdrawn

Case 2: C1, C2, C3, S5 are fully inserted; S4, S6 are fully withdrawn

Case 3: All rods are fully inserted

Cases 4-6: All rods are fully withdrawn

The subcriticality $-\rho = (1 - k_{\text{eff}})/k_{\text{eff}}$, which is the absolute value of negative reactivity ρ, in Cases 1-3 was deduced using (1) the excess reactivity by the positive period method and (2) the control rod worth by the rod-drop method [33]. To convert the dollar unit of subcriticality to the $\Delta k/k$ unit, the effective delayed neutron fraction β_{eff} for each of experimental cores was evaluated using MCNP6.1 [34] with JENDL-4.0 [35].

On the other hand, the subcriticality in Cases 4-6 was not directly measured by the positive period and rod-drop methods, since Cases 4-6 were too deep subcritical systems to reach the critical state for the positive period and the rod-drop methods. For these deep subcritical cores, the prompt neutron decay constant α was directly measured by the PNS method [9] and the Feynman-α method [10], where the spallation neutrons were generated by the combination of the FFAG accelerator and the solid Pb-Bi target. The main characteristics of proton beams were as follows: 100 MeV energy, 1 nA intensity, 20 Hz beam repetition, and 50 ns beam width. In the PNS method and the Feynman-α method, three optical fiber detectors (#1-3 in **Figure 1**) were used to obtain the time-series data of neutron count rate [36]. Note that the experiments by the PNS method and the Feynman-α method were also conducted for Cases 1-3, *i.e.* experimental values of α are available for Cases 1-6 [7].

3. Numerical analysis

3.1. Calculation theory for prompt neutron decay constant

In this section, the calculation theory for prompt neutron decay constant α is briefly explained. The experimental values of α are useful for the validation of prompt ω-eigenvalue calculation. For example, deterministic neutron transport codes such as DANTSYS [37] and PARTISN [31] have a function to search the "time absorption" eigenvalue.

In a strict sense, the prompt neutron decay constant α corresponds to the most negative eigenvalue of spatial and energetic fundamental mode for the natural ω-eigenvalue equation, which includes not only prompt but also delayed neutron production effects [38,39]:

$$\frac{\omega}{\mathrm{v}_g}\psi_g = \left(-\mathbf{A} + \mathbf{F}_p + \sum_{i=1}^{6}\frac{\lambda_i}{\omega+\lambda_i}\mathbf{F}_i\right)\psi_g, \tag{1}$$

where ψ_g and v_g are neutron flux and velocity of the gth energy-group; $\mathbf{A}$, $\mathbf{F}_p$, and $\mathbf{F}_i$ are net loss (leakage and net absorption), prompt neutron production, and the ith precursor-group delayed neutron production operators, respectively; λ_i is the decay constant of the ith precursor. **Equation (1)** can be derived from the time-dependent neutron transport equation under the asymptotic condition where temporal variations of neutron flux and number densities of precursors are proportional to the single-term exponential, $\exp(\omega t)$, after injection of a PNS. Note that the value of α means an exponential decay constant of neutron flux, or $\psi_g \propto \exp(-\alpha t)$, thus α corresponds to the absolute value of ω in this paper, *i.e.* $\alpha \equiv -\omega$.

Let us consider about a deep subcritical state and/or a harder neutron spectrum such as $\alpha > 1000$ [1/s]. Then, since $\alpha \gg \max(\lambda_i) \approx 10$ [1/s], *i.e.* $\frac{\lambda_i}{\omega+\lambda_i} \ll 1$, **Equation (1)** can be well approximated by the following "prompt ω-eigenvalue equation:"

$$\frac{\omega_p}{\mathrm{v}_g}\psi_{g,p} = \left(-\mathbf{A} + \mathbf{F}_p\right)\psi_{g,p}, \tag{2}$$

where the subscript p indicates the prompt ω-mode. Since experimental values of α for Cases 4-6 are $\alpha > \sim 1000$ [1/s] [7], the approximation of **Equation (2)** is reasonable. Consequently, based on **Equation (2)**, α can be obtained as the ω_p-eigenvalue of fundamental mode using the existing codes such as DANTSYS and PARTISN.

3.2. Two-step calculation scheme

In this study, neutronics parameters were evaluated by deterministic codes with a two-step calculation scheme, *i.e.* the lattice calculation using SCALE6.2.1/NEWT [30] followed by the core calculation using PARTISN [31].

3.2.1. Lattice calculation

As shown in **Figure 3**, two types of 2D multi-assemblies models were numerically analyzed by conventional k_{eff}-eigenvalue calculations using NEWT to obtain 7-energy-group homogenized cross sections for 1) fuel assembly, 2) reflector, 3) neutron absorber region in control rod (B_2O_3 for rod-in case or air for rod-out case), and 4) other region around the neutron absorber region (air and aluminum sheaths). Note that *x*- and *z*-axes in **Figure 3** correspond to the radial and the axial directions in the KUCA core, respectively. In **Figure 3**, only right boundary condition is vacuum and others are reflective. These two types of lattices correspond to a) center region and b) upper or lower core-region, respectively.

<Figure 3>

The ENDF/B-VII.1 252-group neutron library (xn252v7.1) were used in these lattice calculations [40]. The resonance calculation for each of unit cells was performed by the ultra-fine group calculation using CENTRM for the following 1D slab geometry: (1) HEU 1/16” thick and polyethylene 3/8” thick, (2) HEU 1/8” thick and Pb-Bi and (3) HEU 1/8” thick and polyethylene 1/8” thick.

In the NEWT calculation, the *x*-directional length for fuel region was adjusted to reproduce the mean chord length $l = 4V/S$ in the actual 3D geometry, where V and S are volume and surface area of fuel plate, respectively. For other regions, the *x*-directional spatial lengths were adjusted to preserve the volume ratios with respect to the fuel region. The spatial

mesh-lengths for *x*- and *z*-directions are smaller than 0.5 cm. As an angle quadrature set, a square Chebychev-Legendre set was used, where the numbers of polar and azimuthal directions are 5 and 9 per octant, respectively. The P_5 scattering was applied in all of materials. Through the lattice calculation using NEWT, 7-energy-group homogenized cross sections were obtained, where the collapsed 7-energy-group structure is shown in **Table 1**. If finer energy group structure is used, discretization error due to energy-group could be reduced, however it requires longer calculation time in the random sampling technique. Thus, based on the verification results as shown in later **Section 4.1.1**, it was judged that the 7-energy-group calculation was practically reasonable for UQ using the random sampling technique.

<Table 1>

3.2.2. Core calculation

Using these 7-energy-group homogenized cross sections, core calculations in 3D geometry were performed by the PARTISN code. **Figure 4** shows an example of calculation geometry and spatial meshes for Case 4. Due to limitations of calculation memory and time, targets of core calculations were only for Cases 3-6 where the control rod patterns are symmetry, *i.e.* total number of spatial meshes were reduced by utilizing the symmetry for *x*- and *z*-axes. The 3D core geometry was divided by approximately $1 \times 1 \times 1\text{cm}$ meshes with 1/4 core symmetry. Instead of treating higher P_L scattering, transport cross section $\Sigma_{\text{tr},g}$ was used. The EO_{16} quadrature set were used as the S_N quadrature [41]. Convergence criteria for inner and outer iterations were 10^{-6}. Additional explanations in the calculation of k_{eff}, one-point kinetics parameters, and α are described in **Sections 3.3.1, 3.3.2, and 3.3.3**, respectively.

<Figure 4>

3.3. Calculation of neutronics parameters

3.3.1. Effective neutron multiplication factor

The effective neutron multiplication factor k_{eff} was estimated using the total fission spectrum χ_g. The total fission spectrum χ_g was obtained by:

$$\chi_g = \left(1 - \sum_{i=1}^{6} \beta_i\right) \chi_{p,g} + \sum_{i=1}^{6} \beta_i \chi_{i,g}, \tag{3}$$

where β_i and $\chi_{i,g}$ are the *i*th precursor-group delayed neutron fraction and fission spectra, respectively. Note that, in the output of homogenized cross section by NEWT, only prompt fission spectrum $\chi_{p,g}$ was provided. To correct the delayed fission spectrum terms, it was assumed that ^{235}U was the main contribution to fission because HEU is used as the fuel at KUCA. The data of $\chi_{i,g}$ were quoted from ENDF/B-VII.1 [40]. The effective neutron multiplication factor k_{eff} and the corresponding scalar flux ϕ_g can be numerically obtained by PARTISN with input of "ievt=1 (k_{eff})".

3.3.2. One-point kinetics parameters

To obtain the one-point kinetics parameters (effective delayed neutron fraction β_{eff}, prompt neutron lifetime ℓ, and neutron generation time Λ), adjoint flux for k_{eff}-eigenvalue calculation is essential. The adjoint scalar flux $\phi_g^{\dagger}$ can be also obtained by PARTISN with inputs of "ievt=1" and "ith=1 (adjoint)". As the results of forward and adjoint k_{eff}-eigenvalue calculations, forward and adjoint flux files (rtflux and atflux) were outputted as binary files. By reading these flux files, β_{eff}, Λ and ℓ were estimated by the following conventional definitions:

$$\beta_{\text{eff}} = \frac{\sum_{i=1}^{6} \langle \phi_g^{\dagger} \mathbf{F}_i \phi_g \rangle}{\langle \phi_g^{\dagger} \left(\mathbf{F}_p + \sum_{i=1}^{6} \mathbf{F}_i \right) \phi_g \rangle}, \tag{4}$$

$$\Lambda = \frac{\langle \frac{\phi_g^\dagger \phi_g}{\mathrm{v}_g} \rangle}{\langle \phi_g^\dagger \left(\mathbf{F}_p + \sum_{i=1}^{6} \mathbf{F}_i \right) \phi_g \rangle}, \tag{5}$$

$$\ell = k_{\mathrm{eff}}\, \Lambda, \tag{6}$$

where bracket $\langle\rangle$ represents integration over all phase space. Note that the higher order flux moments were approximately neglected in the numerator of **Equation (5)**, *i.e.* forward and adjoint scalar fluxes were utilized to estimate Λ and ℓ.

3.3.3. Prompt neutron decay constant

The ω_p-eigenvalue calculation was carried out by PARTISN with input of "ievt=2 (alpha search)". To obtain a negative value of ω_p, or prompt neutron decay constant α, minor modification of the PARTISN source code (tnewpa3d.f) was necessary. The validity of this modification was confirmed by comparing numerical results of α using DANTSYS [37] with the same input files. For α search calculation, production cross section $\nu\Sigma_{\mathrm{f},g}$ for each fuel region was multiplied by $(1 - \sum_{i=1}^{6} \beta_i)$ to generate prompt neutrons only. As the prompt fission spectrum, NEWT outputs of $\chi_{p,g}$ were used as is.

3.4. Uncertainty quantification

3.4.1. Random sampling technique

Once the NEWT/PARTISN analysis scheme is established, the UQ for neutronics parameters can be achieved by the random sampling technique using SCALE6.2.1/Sampler [13,21]. By the aid of Sampler module, random samples of homogenized cross section data, $\boldsymbol{\Sigma}_n$ $(1 \leq n \leq 400)$, were easily obtained by calling the NEWT module for each randomly sampled library data, which are perturbed based on the 56-energy-group covariance library (56groupcov7.1) [13]. Here, homogenized cross section data consists of macroscopic absorption, production, transport and scattering cross sections ($\Sigma_{\mathrm{a},g}, \nu\Sigma_{\mathrm{f},g}, \Sigma_{\mathrm{tr},g}, \Sigma_{\mathrm{s},g\to g'}$), prompt fission spectrum ($\chi_{p,g}$), delayed neutron fractions (β_i), and neutron velocity (v_g). In the

Sampler procedure, the restart file of unperturbed NEWT calculation was utilized as a first guess of neutron flux to reduce the computational time in NEWT. In this study, total number of random sampling N was 400 because of the limitation of total calculation time. Instead of increasing N, the bootstrap method was utilized to quantify the statistical error of random sampling technique without assumption of normality [42,43]. Here, the total number of bootstrap samples B was 10000.

After the Sampler/NEWT calculations, a series of PARTISN core analyses were carried out for each of random samples of homogenized cross section data $\mathbf{\Sigma}_n$ to obtain corresponding neutronics parameters $\vec{y}_n = \left[k_{\mathrm{eff},n}, \beta_{\mathrm{eff},n}, \ell_n, \Lambda_n, \alpha_n\right]$ as described in **Section 3.3**. Note that forward or adjoint flux file (rtflux or aflux) of unperturbed case was utilized as a first guess to reduce the calculation time of each PARTISN analysis. Finally, uncertainty (standard deviation, s) of neutronics parameter was estimated by the square root of unbiased variance, *i.e.* diagonal element of covariance matrix $\mathrm{cov}(\vec{y}, \vec{y})$.

3.4.2. UQ of k_{eff} using perturbation theory

To verify the UQ methodology using the random sampling technique, nuclear data-induced uncertainty of k_{eff} using SCALE6.2.1/TSUNAMI-3D [32] was additionally evaluated as the reference value of uncertainty of k_{eff}. In TSUNAMI-3D, continuous energy Monte Carlo calculation was performed by KENO-V.a with the ENDF/B-VII.1 library [40]. The CLUTCH method was used for the SA to reduce computational memories. The neutron histories per generation (npg), total number of generations (gen), and skip generations (nsk) are 40000, 5400, and 400, respectively. In the CLUTCH method, $F^*(\vec{r})$ meshes, which are used for adjoint weighted tallies for SA, were spatially divided by approximately $1 \times 1 \times 1\mathrm{cm}$ cell units for fuel regions. As a covariance of nuclear data, 56-energy-group covariance library (56groupcov7.1) was used [13].

4. Results and Discussion

4.1. Nuclear data-induced uncertainty

Table 2 shows results of sample mean and relative uncertainty $\equiv \frac{\text{standard deviation}}{\text{sample mean}}$ by the random sampling technique using Sampler/NEWT/PARTISN. In **Table 2**, bracket $[lower, upper]$ means 95% confidence interval estimated by the bootstrap method. By the Shapiro-Wilk [44] and the Jarque-Bera normality tests [45], the null-hypothesis that sample follows a normally distributed population is rejected only for Λ in Cases 3-6 because p-values are smaller than the significance level of 5%. Thus, the bootstrap method was utilized to estimate the confidence intervals as the statistical errors of sample mean and relative uncertainty.

<Table 2>

4.1.1. Verification of random sampling technique

In this section, the verification of UQ methodology using the random sampling technique is described. **Table 3** summarizes numerical results with their statistical errors using SCALE6.2.1/TSUNAMI-3D. It is noted that the normality for the random samples of k_{eff} in Cases 3-6 is checked by the Shapiro-Wilk [44] and the Jarque-Bera normality tests [45], thus the non-linearity effect of k_{eff} to nuclear data seems to be not strong, *i.e.* it is reasonable that the uncertainty by TSUNAMI-3D, which is based on the first-order perturbation theory, is regarded as the reference value to verify the random sampling technique. By comparing between **Tables 2 and 3**, the relative uncertainty of k_{eff} using the random sampling technique is nearly equal to that of TSUNAMI-3D within the range of 95% bootstrap confidence interval. Consequently, it is demonstrated that the random sampling scheme works well.

As a supplement, the experimentally-deduced subcriticality value for Case 3 is $-\rho = 2483 \pm 6$ [pcm], or $k_{\text{eff}} = 0.97577 \pm 0.00006$, according to the reference [7]. Thus, C/E values for sample mean of Sampler/NEWT/PARTISN and KENO-V.a are 0.999 and 1.004,

respectively. There are significantly systematic differences (several hundreds pcm) of k_{eff} between the sample mean of Sampler/NEWT/PARTISN and KENO-V.a, because of the analytical modeling errors, *e.g.* discretization errors of space $\vec{r}$, energy E and direction $\vec{\Omega}$.

<Table 3>

4.1.2. Discussion on subcriticality dependency of α-uncertainty

As shown in **Table 2**, the relative uncertainties of k_{eff} and one-point kinetics parameters (β_{eff}, ℓ, and Λ) are relatively constant against the subcriticality change (Cases 3-6). On the other hand, relative uncertainties of prompt neutron decay constant s_α/α decreases as the subcriticality becomes deeper.

In order to discuss the reason for the tendency of s_α/α, let us consider the approximate expression of α. In the one-point reactor approximation, fundamental mode of eigenvalue α is approximated by

$$\alpha \approx \frac{\beta_{\text{eff}} - \rho}{\Lambda}. \tag{7}$$

Although the actual values of α were estimated by the ω_p-eigenvalue calculation, **Equation (7)** seems to be a reasonable rough estimate for the discussion purpose, because the values of $(\beta_{\text{eff}} - \rho)/\Lambda$ for Cases 3-6 are 717, 1108, 1977 and 2243 [1/sec], which are roughly equal to the α values shown in Table 2. **Equation (7)** shows that the magnitude of α changes according to the variations of β_{eff}, $-\rho$, and Λ originated from the nuclear data. Thus, the nuclear data-induced uncertainty s_α can be indirectly estimated through the nuclear data-induced uncertainties of β_{eff}, $-\rho$, and Λ. Based on the uncertainty propagation for **Equation (7)**, the magnitude of s_α/α is approximately estimated by

$$\frac{s_\alpha}{\alpha} \approx \sqrt{\begin{array}{l}\left(\frac{s_\beta}{\beta_{\text{eff}}-\rho}\right)^2+\left(\frac{s_{-\rho}}{\beta_{\text{eff}}-\rho}\right)^2+\left(-\frac{s_\Lambda}{\Lambda}\right)^2 \\ +2\left(\frac{s_\beta}{\beta_{\text{eff}}-\rho}\right)\left(\frac{s_{-\rho}}{\beta_{\text{eff}}-\rho}\right)\text{cor}(\beta_{\text{eff}},-\rho) \\ +2\left(\frac{s_\beta}{\beta_{\text{eff}}-\rho}\right)\left(-\frac{s_\Lambda}{\Lambda}\right)\text{cor}(\beta_{\text{eff}},\Lambda) \\ +2\left(\frac{s_{-\rho}}{\beta_{\text{eff}}-\rho}\right)\left(-\frac{s_\Lambda}{\Lambda}\right)\text{cor}(-\rho,\Lambda)\end{array}}, \quad (8)$$

where s_β, $s_{-\rho}$ and s_Λ are nuclear data-induced uncertainties of β_{eff}, $-\rho$ and Λ, respectively; $\text{cor}(x,y)$ is nuclear data-induced correlation coefficient between x and y. In the order of Cases 3-6, the magnitude of each term in **Equation (8)** was calculated as follows: $s_{-\rho}/(\beta_{\text{eff}}-\rho)$ are 28, 18, 10 and 9%; $s_\beta/(\beta_{\text{eff}}-\rho)$ are 0.72, 0.43, 0.23, and 0.20%; and s_Λ/Λ are 1.10, 1.26, 1.31, and 1.32%, respectively. Compared with $s_{-\rho}/(\beta_{\text{eff}}-\rho)$, the magnitudes of $s_\beta/(\beta_{\text{eff}}-\rho)$ and s_Λ/Λ are relatively small to be negligible, even if the correlation terms ($\text{cor}(\beta_{\text{eff}},-\rho)\approx+0.2$, $\text{cor}(\beta_{\text{eff}},\Lambda)\approx+0.2$ and $\text{cor}(-\rho,\Lambda)\approx+0.8$) are taken into account. Namely, **Equation (8)** is further approximated by

$$\frac{s_\alpha}{\alpha} \approx \frac{s_{-\rho}}{\beta_{\text{eff}}-\rho}. \quad (9)$$

In fact, $s_{-\rho}/(\beta_{\text{eff}}-\rho)$ are almost the same as the relative uncertainties of α in **Table 2**. Thus, it is supposed that the nuclear data-induced uncertainty $s_{-\rho}/(\beta_{\text{eff}}-\rho)$ is the major indirect contribution to s_α/α, *i.e.* the tendency of s_α/α is similar to that of $s_{-\rho}/(\beta_{\text{eff}}-\rho)$. While the absolute uncertainties of $s_{-\rho}$ are approximately the same for Cases 3-6 ($s_{-\rho}\approx 0.01$), the value of $\beta_{\text{eff}}-\rho$ increases as the subcriticality deepen. Consequently, s_α/α approximately decreases in inverse proportional to the value of $-\rho$.

4.1.3. Comparison of α with experimental results

Table 4 shows the experimental results of prompt neutron decay constant with their fitting errors for Cases 3-6 which are quoted from reference [7]. In **Table 4**, a number in the parentheses represents a standardized difference between experimental value (α_{exp}) and the

sample mean of Sampler/NEWT/PARTISN ($\bar{\alpha}$), which is normalized by the nuclear data-induced uncertainty (s_α):

$$d \equiv \frac{\alpha_{\text{exp}} - \bar{\alpha}}{s_\alpha}. \tag{10}$$

By compared between **Tables 2** and **4**, it is confirmed that the numerical results of α agree well with the experimental ones within the 1σ ranges of nuclear data-induced uncertainties, for Fibers #1 and #2 by the PNS method.

For other cases, the standard differences are approximately within the 3σ ranges. The differences by the Feynman-α method seems to be larger than those of the PNS method, which implies that potential experimental errors of Fibers #1-3 using the Feynman-α method might be larger, *e.g.* systematic errors due to low removal efficiency for spatial higher mode components in the fitting process to estimate α. The exhaustive quantification of such experimental errors is one of the future studies. In addition, as shown in **Figure 1**, the position of Fiber #3 is close to the spallation neutron source due to Pb-Bi target. Thus, the spallation neutron source influences on the experimental values of Fiber #3, which results in larger variations of standardized differences against the subcriticality change, as compared with Fibers #1 and #2.

<Table 4>

4.2. Nuclear data-induced correlation

Using the results of random samples of neutronics parameters $\vec{y}_n = \left[k_{\text{eff},n}, \beta_{\text{eff},n}, \ell_n, \Lambda_n, \alpha_n\right]$, nuclear data-induced correlation coefficient matrix among them are estimated.

<Figure 5>

As shown in **Figure 5**, Cases 3-6 are very strongly correlated to each other, although core geometries are different among them. In addition, it is noted that the correlation coefficients are very strongly negative (≈ -1) between α and k_{eff}; and strongly positive ($\approx +0.8$) between α and Λ. Such strong correlation implies that numerical predictions of k_{eff} and Λ can be improved by a data assimilation technique using experimental values of α for subcritical systems, where it is noted that the prompt neutron decay constant α can be directly measured using the PNS method or the Feynman-α method even for a deep subcritical experimental core. Examples of the data assimilation techniques are the bias factor method [46] and the cross section adjustment technique [47]. As discussed in previous study [46], experimental values, which have strong correlation with target parameters, are very useful information to reduce the uncertainties of predicted target parameters. One of the future studies is application of the data assimilation technique using measured α to accurately predict other neutronics parameters such as k_{eff} and one-point kinetics parameters. For this purpose, the challenging issues are to appropriately estimate covariance matrices of analytical modeling errors (*e.g.* discretization errors in deterministic codes) for neutronics parameters and to exhaustively evaluate the experimental errors.

5. Conclusions

Nuclear data-induced uncertainties of neutronics parameters (neutron multiplication factor k_{eff}, one-point kinetics parameters and prompt neutron decay constant α) were quantified for the Pb-Bi zoned ADS experiments at KUCA. As a first attempt for UQ of these parameters, the random sampling technique was applied to two-step (lattice-core) calculation scheme. The UQ using the random sampling technique was accomplished by SCALE6.2.1/Sampler/NEWT/PARTISN, of which methodology was verified by comparing with reference values of nuclear data-induced uncertainties of k_{eff} using

SCALE6.2.1/TSUNAMI-3D.

Consequently, it was confirmed that the relative uncertainties of k_{eff} and one-point kinetics parameters (β_{eff}, ℓ, and Λ) are relatively constant against the subcriticality change of experimental cores. On the other hand, relative uncertainty of prompt neutron decay constant decreases as the subcriticality becomes deeper, because the nuclear data-induced uncertainty of subcriticality is the major indirect contribution to the uncertainty of α. In this study, numerical values α were estimated as the ω_p-eigenvalue of fundamental mode using PARTISN. The results of α reasonably agree with the experimental values, compared with nuclear data-induced uncertainties by the random sampling technique. Furthermore, it was clarified that there are strong correlations between α and k_{eff} and between α and Λ. This fact implies that the numerical predictions of k_{eff} and Λ can be improved by the data assimilation technique using subcritical experimental results such as α, which can be directly measured.

References

[1] Pyeon CH, Misawa T, Lim JY, et al. First injection of spallation neutrons generated by high-energy protons into the Kyoto University Critical Assembly. J Nucl Sci Technol. 2009;46:1091-1093.

[2] Pyeon CH, Shiga H, Abe K, et al. Reaction rate analysis of nuclear spallation reactions generated by 150, 190, and 235MeV protons. J Nucl Sci Technol. 2010;47:1090-1095.

[3] Lim JY, Pyeon CH, Yagi T, et al. Subcritical multiplication parameters of the accelerator-driven system with 100 MeV protons at the Kyoto University Critical Assembly. Sci Technol Nucl Install. 2012;2012:395878.

[4] Pyeon CH, Azuma T, Takemoto Y, et al. Experimental analyses of spallation neutrons generated by 100 MeV protons at the Kyoto University Critical Assembly. Nucl Eng Technol. 2013;45:81-88.

[5] Pyeon CH, Nakano H, Yamanaka M, et al. Neutron characteristics of solid targets in accelerator-driven system with 100-MeV protons at Kyoto University Critical Assembly. Nucl Technol. 2015;192:181-190.

[6] Pyeon CH, Fujimoto A, Sugawara T, et al. Validation of Pb nuclear data by Monte Carlo analyses of sample reactivity experiments at Kyoto University Critical Assembly. J Nucl Sci Technol. 2016;53:602-612.

[7] Pyeon CH, Yamanaka M, T. Endo, et al. Experimental benchmarks on kinetic parameters in accelerator-driven system with 100 MeV protons at Kyoto University Critical Assembly. Ann Nucl Energy. 2017;105:346-354.

[8] Pyeon CH, Yamanaka M, Kim SH. Benchmarks of subcriticality in accelerator-driven system at Kyoto University Critical Assembly. Nucl Eng Technol. 2017;49:1234-1239.

[9] Simmons BE, King JS. A pulsed technique for reactivity determination. Nucl Sci Eng. 1958;3:595-608.

[10] Kitamura Y, Pázsit, I, Wright J, et al. Calculation of the pulsed Feynman- and Rossi-alpha

formulae with delayed neutrons. Ann Nucl Energy. 2005;32:671-692.

[11] Lagrange JB, Planche T, Yamakawa E, et al. Straight scaling FFAG beam line. Nucl Instrum Methods Phys Res A. 2012;691:55-63.

[12] Yamakawa E, Uesugi T, Lagrange JB, et al. Serpentine acceleration in zero-chromatic FFAG accelerators. Nucl Instrum Methods Phys Res A. 2013;716:46-53.

[13] Rearden BT, Jessee MA. SCALE code system. Oak Ridge (TN): Oak Ridge National Laboratory; 2016, ORNL/TM-2005/39 Version 6.2.1.

[14] Hara A, Takeda T, Kikuchi Y. SAGEP: Two-dimensional sensitivity analysis code based on generalized perturbation theory. Ibaraki (Japan): Japan Atomic Energy Agency; 1984, JAERI-M 84-027.

[15] Yokoyama K, Jin T, Hirai Y, et al. Development of the versatile reactor analysis code system, MARBLE2. Ibaraki (Japan): Japan Atomic Energy Agency; 2015, JAEA-Data/Code 2015-009.

[16] Chiba G, Pyeon CH, van Rooijen WFG, et al. Nuclear data-induced uncertainty quantification of neutronics parameters of accelerator-driven system. J Nucl Sci Technol. 2016;53:1653-1661.

[17] Chiba G, Tsuji M, Sugiyama K, et al. JENDL-4.0 benchmarking for effective delayed neutron fraction of fast neutron systems. J Nucl Sci Technol. 2011;48:1471-1477.

[18] Kodeli IA, Sensitivity and uncertainty in the effective delayed neutron fraction (β_{eff}), Nucl Instrum Methods Phys Res A, 2013;715:70-78.

[19] Chiba G, Tsuji M, Narabayashi T. Uncertainty quantification of reactor kinetics parameters using JENDL-4.0 covariance data. Proc PHYSOR 2014; 2014 Sep 28-Oct 3; Kyoto (Japan). [CD-ROM].

[20] Rochman D, Koning AJ, van der Marck SC, et al. Nuclear data uncertainty propagation: Perturbation vs. Monte Carlo. Ann Nucl Energy. 2011;38:942-952.

[21] Williams ML, Ilas G, Jessee MA, et al. A statistical sampling method for uncertainty

analysis with SCALE and XSUSA. Nucl Technol. 2013;183:515-526.

[22] Wieselquist W, Zhu T, Vasiliev A, et al. PSI methodologies for nuclear data uncertainty propagation with CASMO-5M and MCNPX: Results for OECD/NEA UAM benchmark phase I. Sci Technol Nucl Install. 2013;2013:549793.

[23] Zwermann W, Aures A, Gallner L, et al. Nuclear data uncertainty and sensitivity analysis with XSUSA for fuel assembly depletion calculations. Nucl Eng Technol. 2014;46:343-352.

[24] Yamamoto A, Kinoshita K, Watanabe T, et al. Uncertainty quantification of LWR core characteristics using random sampling method. Nucl Sci Eng. 2015;181:160-174.

[25] Díez CJ, Buss O, Hoefer A, et al. Comparison of nuclear data uncertainty propagation methodologies for PWR burn-up simulations. Ann Nucl Energy. 2015;77:101-114.

[26] Fiorito L, Griseri M, Stankovskiy A. Nuclear data uncertainty propagation in reactor studies using the SANDY Monte Carlo sampling code. Proc M&C 2017; 2017 Apr 16-20; Jeju (Korea). [USB].

[27] Fiorito L, Buss O, Hoefer Axel, et al. Decay heat uncertainty quantification of MYRRHA. EPJ Web Conf ND2016. 2017;146:09021.

[28] Rochman D, Leray O, Hursin M, et al. Nuclear data uncertainties for typical LWR fuel assemblies and a simple reactor core. Nucl Data Sheets. 2017;139:1-76.

[29] Leray O, Fiorito L, Rochman D, et al. Uncertainty propagation of fission product yields to nuclide composition and decay heat for a PWR UO2 fuel assembly. Prog Nucl Energy. https://doi.org/10.1016/j.pnucene.2017.05.033

[30] Dehart MD. Advancements in generalized-geometry discrete ordinates transport for lattice physics calculations. Proc PHYSOR-2006; 2006 Sep 10-14; Vancouver (Canada). [CD-ROM].

[31] Alcouffe RE, Baker RS, Dahl JA, et al. PARTISN: A time-dependent, parallel neutral particle transport code system. Los Alamos (NM): Los Alamos National Laboratory; 2008,

LA-UR-08-07258.

[32] Perfetti CM, Rearden BT, Martin WR. SCALE continuous-energy eigenvalue sensitivity coefficient calculations. Nucl Sci Eng. 2016;182:332-353.

[33] Misawa T, Unesaki H, Pyeon CH. Nuclear Reactor Physics Experiments. Japan: Kyoto University Press; 2010.

[34] Goorley JT, James MR, Booth TE, et al. Initial MCNP6 release overview -MCNP6 version 1.0. Los Alamos (NM): Los Alamos National Laboratory; 2013. LA-UR-13-22934.

[35] Shibata K, Iwamoto O, Nakagawa T, et al. JENDL-4.0: A new library for nuclear science and engineering. J Nucl Sci Technol. 2011;48:1-30.

[36] Yagi T, Pyeon CH, Misawa T, Application of wavelength shifting fiber to subcriticality measurements. Appl Radiat Isot. 2013;72:11-15.

[37] Alcouffe RE, Baker RS, Brinkley FW, et al. DANTSYS: A diffusion accelerated neutral particle transport code system. Los Alamos (NM): Los Alamos National Laboratory; 1995, LA-12969-M.

[38] Henry AF, The application of inhour modes to the description of non-separable reactor transients. Nucl Sci Eng. 1964;20:338-351.

[39] Stacy WM. Space-time nuclear reactor kinetics. New York (NY), Academic Press: 1969.

[40] Chadwick MB, Herman M, Obložinský P, et al. ENDF/B-VII.1 nuclear data for science and technology: Cross Sections, covariances, fission product yields and decay data. Nucl Data Sheets. 2011;112:2887-2996.

[41] Endo T, Yamamoto A. Development of new solid angle quadrature sets to satisfy even- and odd-moment conditions. J Nucl Sci Technol. 2007;44:1249-1258.

[42] Efron B, Bootstrap methods: Another look at the Jackknife. Ann Stat. 1979;7:1-26.

[43] Endo T, Watanabe T, Yamamoto A. Confidence interval estimation by bootstrap method for uncertainty quantification using random sampling method. J Nucl Sci Technol. 2015;52:993-999.

[44] Shapiro SS, Wilk MB. An analysis of variance test for normality (complete samples). Biometrika. 1965;52:591-611.

[45] Jarque CM, Bera AK. A test for normality of observations and regression residuals. Int Stat Rev. 1987;55:163-172.

[46] Endo T, Yamamoto A, Watanabe T. Bias factor method using random sampling technique. J Nucl Sci Technol. 2016;53:1494-1501.

[47] Watanabe T, Endo T, Yamamoto A, et al. Cross section adjustment method based on random sampling technique. J Nucl Sci Technol. 2014;51:590-599.

Figure captions

Table captions

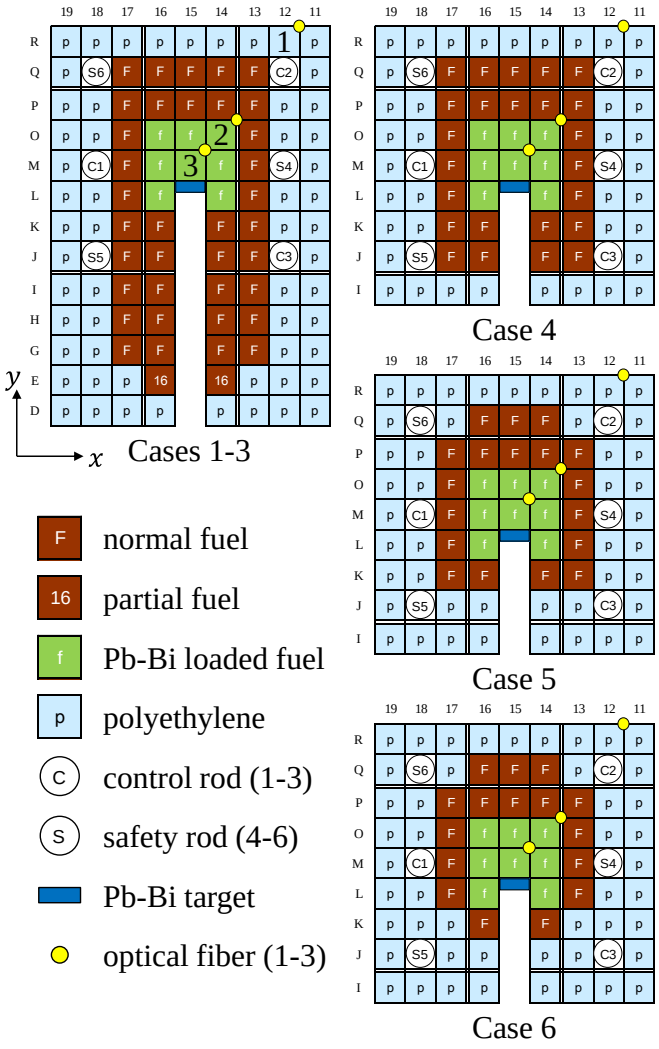

Figure 1. Top view of Pb-Bi zoned experimental cores.

T. Endo:

Experimental analysis and uncertainty quantification using random sampling technique for ADS experiments at KUCA

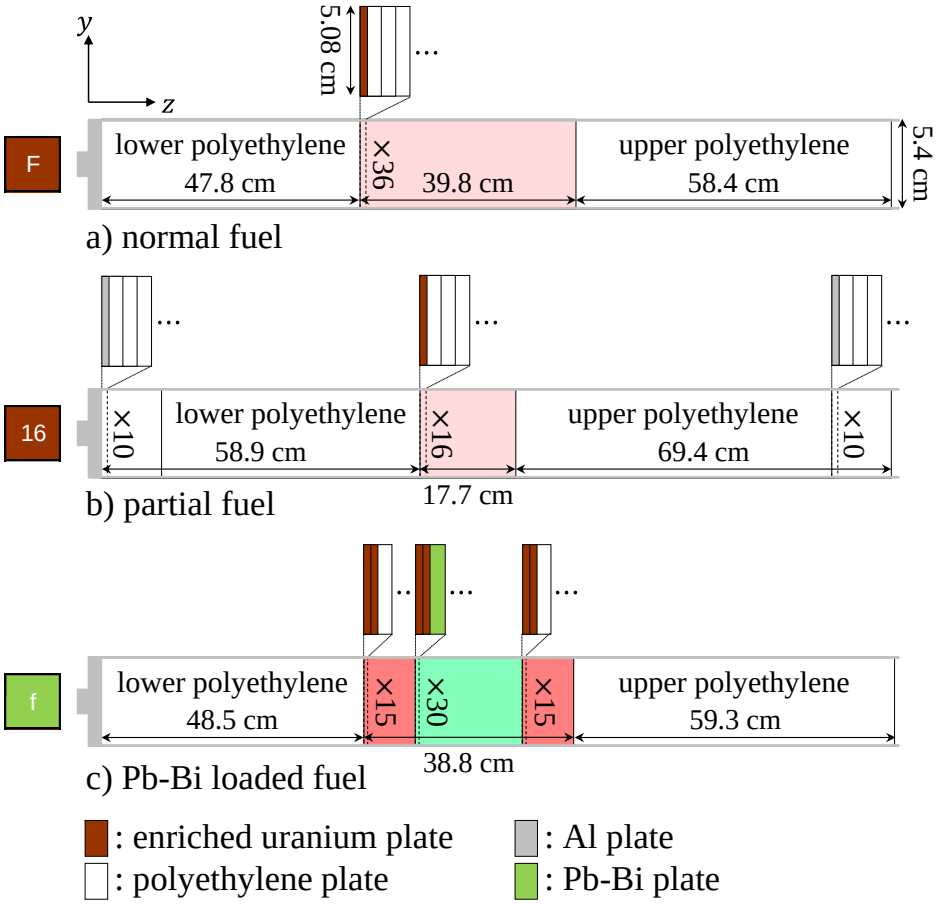

Figure 2. Fuel assemblies loaded in experimental cores.

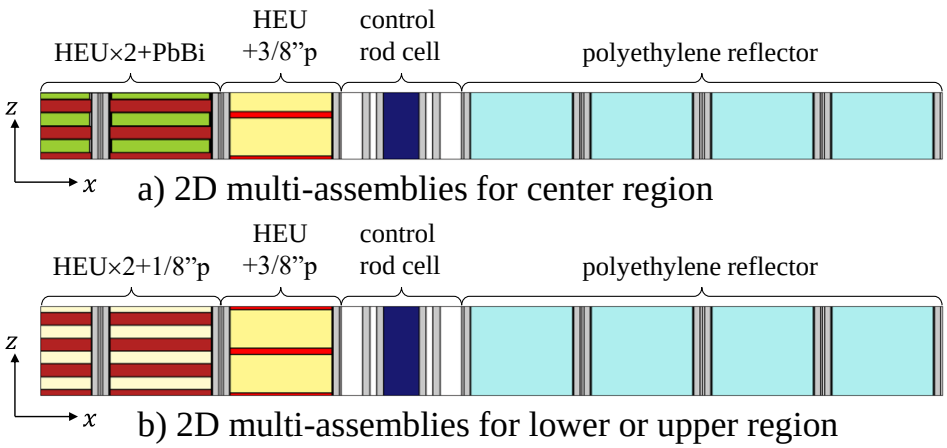

Figure 3. Lattice calculation geometries in NEWT.

T. Endo:

Experimental analysis and uncertainty quantification using random sampling technique for ADS experiments at KUCA

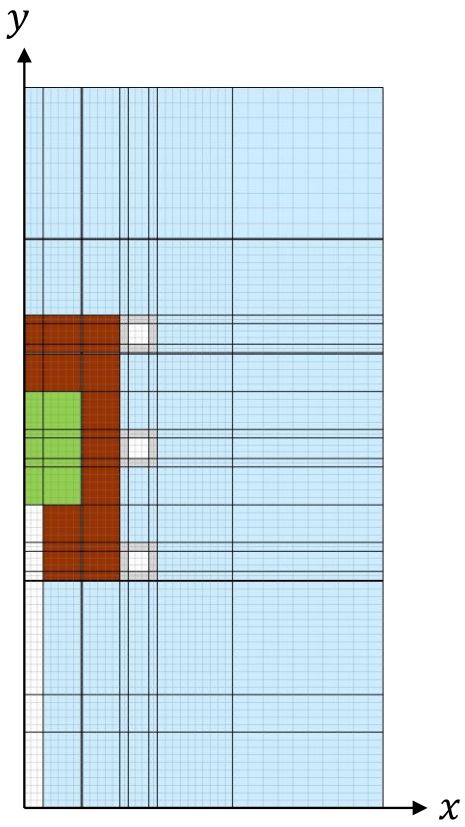

Figure 4. Top view of core calculation geometry (Case 4).

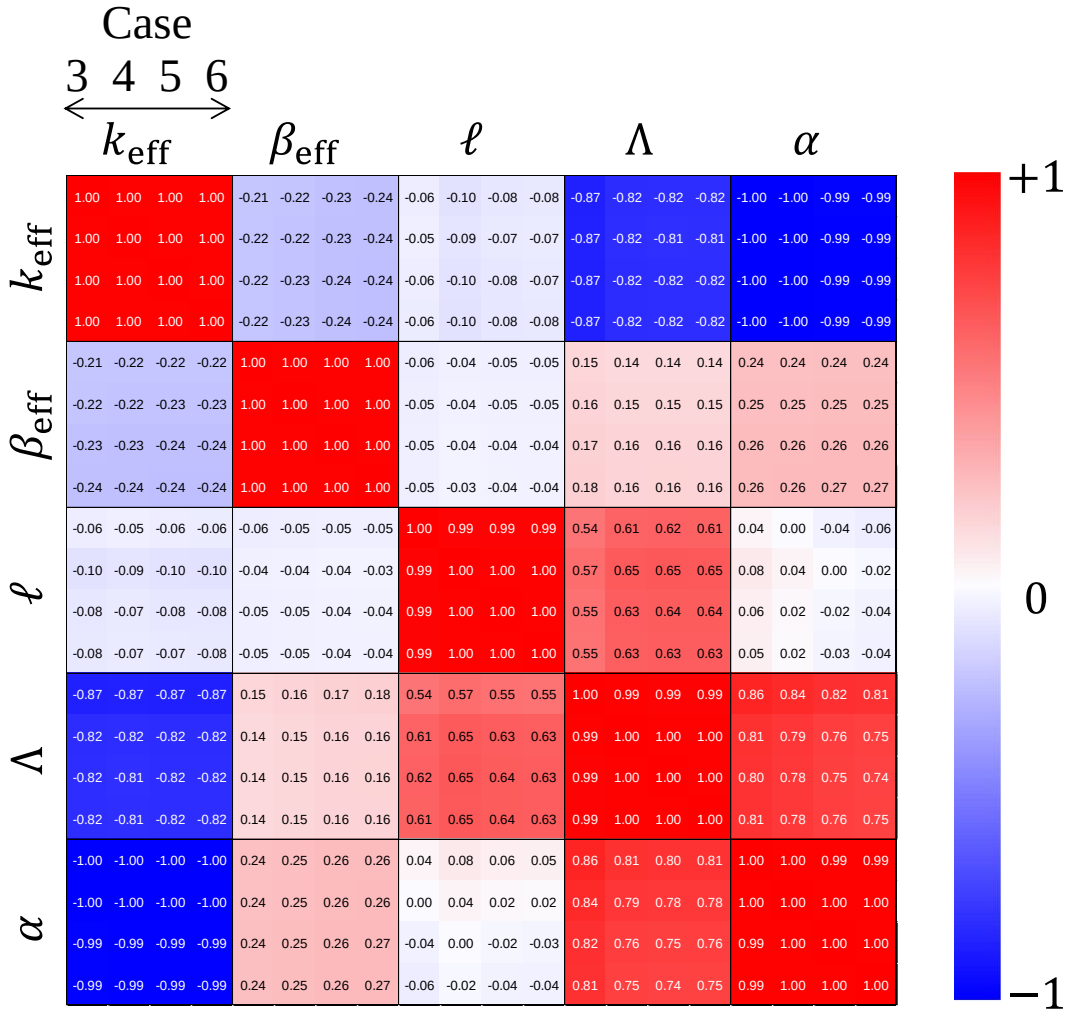

Figure 5. Nuclear data-induced correlation coefficient matrix.

Table 1. Collapsed 7-energy-group structure.

	energy boundary [eV]	
group	upper	lower
1	2.000×10^{7}	1.356×10^{6}
2	1.356×10^{6}	9.500×10^{3}
3	9.500×10^{3}	4.100
4	4.100	6.250×10^{-1}
5	6.250×10^{-1}	1.500×10^{-1}
6	1.500×10^{-1}	5.000×10^{-2}
7	5.000×10^{-2}	1.000×10^{-5}

Table 2. Summary of random sampling technique.

parameter	Case	sample mean		relative uncertainty [%]	
k_{eff} [-]	3	0.9746	[0.9737,0.9755]†	0.92	[0.86,1.01]
	4	0.9532	[0.9523,0.9541]	0.96	[0.90,1.05]
	5	0.9107	[0.9098,0.9116]	1.01	[0.94,1.10]
	6	0.8979	[0.8970,0.8988]	1.02	[0.96,1.11]
β_{eff} [pcm]	3	742	[739,744]	3.25	[3.03,3.51]
	4	747	[745,750]	3.25	[3.03,3.52]
	5	754	[752,757]	3.26	[3.04,3.53]
	6	757	[754,759]	3.26	[3.04,3.53]
ℓ [μs]	3	45.56	[45.54,45.59]	0.54	[0.50,0.58]
	4	48.72	[48.69,48.75]	0.73	[0.68,0.78]
	5	48.64	[48.61,48.68]	0.75	[0.70,0.81]
	6	48.55	[48.51,48.58]	0.75	[0.70,0.81]
Λ [μs]	3	46.75	[46.70,46.80]	1.10	[1.03,1.21]
	4	51.12	[51.05,51.18]	1.26	[1.18,1.39]
	5	53.42	[53.35,53.49]	1.31	[1.22,1.44]
	6	54.07	[54.00,54.14]	1.32	[1.23,1.46]
α [1/s]	3	699	[680,717]	26.85	[24.99,29.27]
	4	1049	[1032,1065]	16.01	[14.94,17.37]
	5	1782	[1768,1797]	8.40	[7.85,9.09]
	6	1996	[1982,2010]	7.28	[6.81,7.87]

† Numbers in brackets correspond to the 95% bootstrap confidence interval for sample mean or relative uncertainty

Table 3. Summary of TSUNAMI-3D.

Case	k_{eff} [-]	relative uncertainty [%$\Delta k/k$]
3	0.97982 ± 0.00006	0.8829 ± 0.0002
4	0.95754 ± 0.00007	0.9184 ± 0.0002
5	0.91297 ± 0.00006	0.9602 ± 0.0002
6	0.89927 ± 0.00007	0.9759 ± 0.0002

Table 4. Measured prompt neutron decay constants for Cases 3-6.

Case	PNS method [1/s]			Feynman-α method [1/s]		
	Fiber #1	Fiber #2	Fiber #3	Fiber #1	Fiber #2	Fiber #3
3	673 ± 4	632 ± 2	1020 ± 8	655 ± 2	620 ± 2	877 ± 5
	(-0.14)†	(-0.36)	(1.71)	(-0.23)	(-0.42)	(0.95)
4	983 ± 4	971 ± 3	1378 ± 18	815 ± 6	822 ± 5	1029 ± 12
	(-0.39)	(-0.46)	(1.95)	(-1.39)	(-1.35)	(-0.12)
5	1665 ± 9	1681 ± 5	1828 ± 23	1365 ± 9	1400 ± 7	1669 ± 17
	(-0.78)	(-0.68)	(0.30)	(-2.78)	(-2.55)	(-0.75)
6	1911 ± 7	1931 ± 3	2061 ± 38	1556 ± 13	1636 ± 10	1917 ± 22
	(-0.59)	(-0.45)	(0.43)	(-3.02)	(-2.47)	(-0.54)

† A number in parentheses represents a standardized difference defined by **Equation (10)**